http://dx.doi.org/10.5012/bkcs.2012.33.8.2483

Articles

Study on the Kinetics and Mechanism of Grain Growth during the Thermal Decomposition of Magnesite

Da-xue Fu, Nai-xiang Feng,* and Yao-wu Wang

School of Materials and Metallurgy, Northeastern University, Shenyang, Liaoning 110819, China
**E-mail: Fengnaixiang@163.com; lllow@126.com*
Received March 22, 2012, Accepted April 2, 2012

The X-ray line broadening technique was used to calculate the grain size of MgO at 1023, 1123, 1223 K respectively either in CO_2 or during the thermal decomposition of magnesites in air as well as in vacuum. By referring to the conventional grain growth equation, $D^n = kt$, the activation energy and pre-exponential factor for the process in air are gained as 125.8 kJ/mol and 1.56×10^8 nm^4/s, respectively. Ranman spectroscopy was employed to study the surface structure of MgO obtained during calcination of magnesite, by which the mechanism of grain growth was analyzed and discussed. It is suggested that a kind of highly reactive MgO is produced during the thermal decomposition of magnesites, which is exactly the reason why the activation energy of the grain growth during the thermal decomposition of magnesite is lower than that of bulk diffusion or surface diffusion.

Key Words : Grain growth, Kinetics, CO_2 adsorption, Highly reactive MgO, Magnesite

Introduction

Active MgO has many industrial applications, such as in agriculture, cattle feed, environmental control, manufacture of special cements and in many other specialty uses.[1] How to get more active magnesium oxide has been the focus of attention. Caustic magnesia, a comparatively more porous and active material can be obtained at relatively low temperatures from calcined magnesite[1-4] or brucit.[5,6] As we know, particle size is one of the factors that affect the activity of MgO. Therefore, it is necessary to study on the grain growth of active MgO during the decomposition of magnesite or brucite. As reported by Y. Kotera *et al.*[7] and K. Alihara and A. C. D. Chaklader,[8] the isothermal kinetics of grain growth of MgO during the decomposition of brucite in air and in the condition of H_2O vapor have been studied. The data they collected were treated by the conventional grain-growth equation $D^n = kt$ and hence the activation energy for this process was gained as 32 kal/mol and 31 kal/mol, respectively, which were lower than that of bulk diffusion[9,10] (79 kal/mol for Mg^{2+} in MgO and 62.4 kal/mol for O^{2-} in MgO) and surface diffusion[11] of MgO (90 kcal/mol). Because of the surface hydroxyl groups[12] generated on MgO in the presence of water vapor, Anderson[13] and Razouk[14] suggested that enhancement occurs because of condensation between surface hydroxyl groups of adjacent crystallites with formation of oxygen bridges, which reduced the activation energy of this process as shown in Figure 1. However, few studies were conducted on the isothermal kinetics of particle growth of active MgO during the calcination of magnesite.

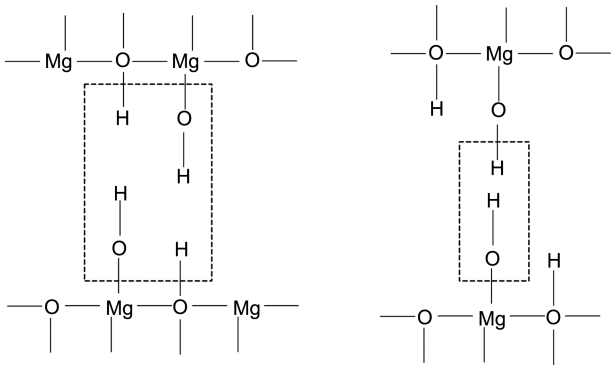

Figure 1. The surface hydroxyl groups on MgO and the formation of oxygen bridges.

On the other hand, as we know, CO_2 is produced during the thermal decomposition of magnesite. Analogous to the surface hydroxyl groups formed on MgO in the presence of water vapor, whether some kinds of surface structure are formed on MgO by the adsorption of CO_2. These surface structures resulted from the adsorption of CO_2 have been relatively well confirmed by several workers[15-19] using the infra-red study as shown in Figure 2. They used the active MgO as the raw material and the adsorption of CO_2 was carried out either at room temperature or at temperature varied from 473 K to 773 K. Four major vibrational frequencies for unidentate carbonates (Figure 2(a)) are assigned at 1510-1550, 1390-1410, 1035-1050, and 860-865 cm^{-1}. Bidentate carbonates (Figure 2(b)) show peaks at 1665-1670, 1325-1330, 1005-1030, and 850-855 cm^{-1}. Vibrational

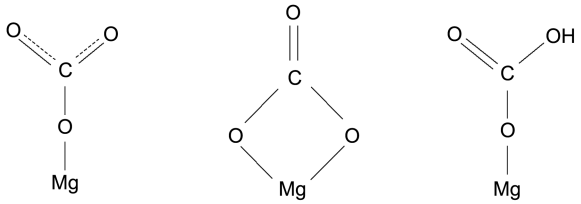

Figure 2. Surface carbonates, formed by adsorption of CO_2 on MgO. (a) unidentate carbonate (b) bidentate carbonate (c) bicarbonate.

frequencies for bicarbonates (Figure 2(c)) are assigned at 1655-1658, 1405-1419 and 1220-1223 cm^{-1}. However, the surface structures of the obtained MgO during calcination of magnesite have been seldom reported in any precedent papers.

In this paper, the isothermal kinetics of grain growth of active MgO during calcination of magnesite are studied and the surface structures of the obtained MgO during calcination of magnesite are investigated. At last, the probable mechanisms of grain growth are discussed.

Materials and Methods

Material. The natural material used in this study was obtained from Dashiqiao, Liaoning Province. The major compositions contained in this material were as follows; 47.28% MgO, 0.56% CaO, 0.24% SiO_2, 0.23% Fe_2O_3, 0.08% Al_2O_3, and 51.27% Ignition loss.

Procedure. The ore was crushed and sieved to –74 μm for the calcination experiment carried out at the temperature of 1023 K, 1123 K, 1223 K, respectively. In the case of calcination of magnesite in the air atmosphere, the sample was placed in a furnace with globar heating elements. The temperature was controlled within ± 5 K by k-type thermocouple placed near the sample. For calcinations in vacuum, a separate steel tube (1Cr25Ni20Si2) with one end closed, was inserted into the furnace and was connected with a mechanical vacuum pump. A constant weight (1.5 g) of magnesite powder was spread uniformly and thinly (1-2 mm thick) on a porcelain boat (ID = 45 mm) and was calcined in the experimental temperature in air and vacuum, up to a period of 30, 60, 90, 120 min, respectively and was air quenched afterward. For the vacuum test, the pressure, which varied from 4Pa to 20Pa, was not strictly controlled since the purpose of this experiment was focused on the comparison of the grain growth between air and vacuum atmosphere.

For experiments in CO_2 atmosphere, a very fine crystallite MgO was chosen as the starting material, which is to void the effect of CO_2 arising from the decomposition reaction of magnesite. The fine crystallite MgO was made by calcining magnesite in vacuum at 853 K for 120 min. As at this temperature the growth rate of MgO particles is very slow, the grain size of MgO obtained was approximate 70 Å. The MgO were subsequently heat treated in CO_2 at 1023 K, 1123 K, 1223 K for 30, 60, 90, 120 min, respectively. The flow rate of CO_2 vapor was 3 L/min.

The samples were not placed into the furnace until the experimental temperature in all the cases. Tests showed that the necessary time for the specimen to reach the furnace temperature was less than one minute. The samples were sealed into the desiccators for particle size measurement.

Particle Size Measurement. The X-ray line broadening technique was mainly used for particle size determination. There were many researchers using this method to study crystallite growth.[20-22] The method was derived by D. Lewis and H. Pearson.[23] The final equation is given as follow:

$$\frac{\beta\cos\theta}{\lambda} = \frac{1}{D} + \frac{2\eta\sin\theta}{\lambda} \quad (1)$$

Where D is the grain size, β is the half intensity width, θ is the Bragg diffraction angle, λ is the wave length of X-ray, and η is the lattice strain. The powders were examined by X-ray diffractometer (PW3040/60 PANALYTICALB Netherlands) using a copper target (K_a) at 40 kV with a scanning speed of 0.03 degrees/sec. The profiles of (200), (220), (222) were chosen to calculate the grain size. The half intensity width β was corrected for the instrumental width employing $\beta^2 = \beta_{ob}^2 - \beta_i^2$, where β_{ob} is the observed half intensity width and β_i is the instrumental half intensity width. In this work, β_i = 0.075°, λ = 1.5406 Å.

Characterization. The grain size of the caustic MgO resulted from the calcined magnesite in air and vacuum was investigated by a scanning electron microscope (SEM, S-4800, HITACHI, Japan).

The change of surface structure during the thermal decomposition of magnesites was characterized by laser Raman spectroscopy. A Kimmon Koha He-Cd UV laser (18 mW, 448.0 nm) and an Olympus UV microscope objective (50 × 0.5) were used. Raman spectra were recorded 2 times with an integration time of 30s by a Horiba Jobin Yvon Labram HR 800 Raman spectrometer.

Raman spectra were acquired at temperatures from ambient temperature to 973 K, in increments of approximately 50 K. Temperature-dependent Raman measurements were performed within a furnace which was shown in Figure 3. A platinum crucible (d5 mm × 6 mm), which was used as the sample holder, placed in a corundum tube. The corundum

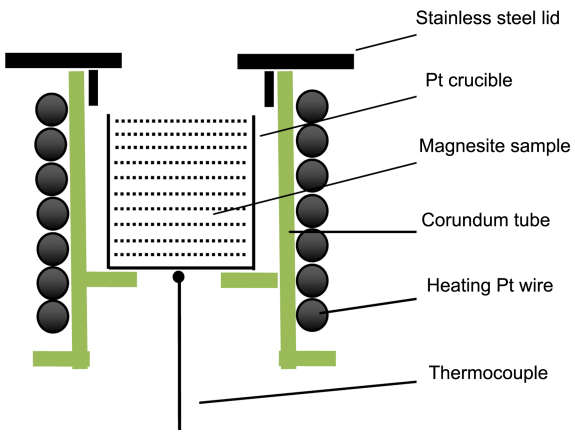

Figure 3. Schematic view of sample cell for temperature-dependent Raman measurements.

tube had an external thread for platinum wire wounding around. A Guolong TCW-32B temperature controller connected to a Pt-PtRh10 type thermocouple was used to control the temperature. A MgO sample was sealed in CO_2 for 30 minutes at room temperature, the surface structure of which was measured thereafter at the room temperature for comparing with the sample in the high temperature.

Results

A plot of $\beta\cos\theta/\lambda$ *vs* $2\sin\theta/\lambda$ for the specimen prepared in air at 1123 K for 60 min is shown in Figure 4. The intercept on the $\beta\cos\theta/\lambda$ axis corresponds to the reciprocal of the particle size whereas the slope indicates the strain in the particle. For this specimen, the particle size calculated from the intercept was 292.5 ± 4.1 Å and the strain obtained from the slope was 1.2% ± 0.07%. The particle size of other specimens was calculated in the same way.

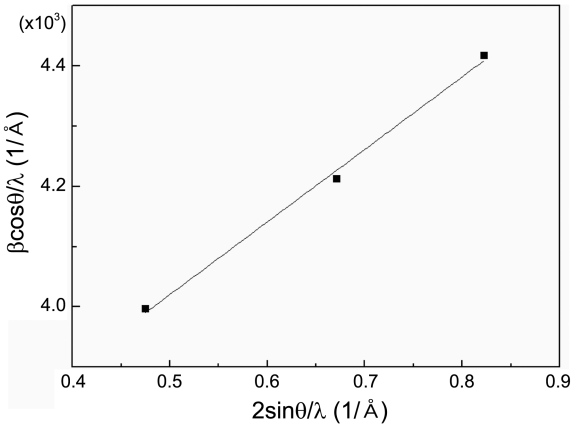

Figure 4. The plot of MgO prepared at 1123 K for 60 min.

The particle size of MgO was determined as a function of time, over the temperature range from 1023 K to 1223 K, in air, vacuum and CO_2. The effect of different environments on the growth of MgO particles during heat treatment is shown in Figure 5.

The particle size was smaller in vacuum than in air at the same decomposition temperature and time, which indicated that the growth of MgO particles was affected by the vacuum. As we know, the thermal decomposition of magnesite is expressed as follows:

$$MgCO_3(s) \xrightarrow{\text{heating}} MgO(s) + CO_2(g) \quad (2)$$

The degassing rate is faster in vacuum than in air. This indicates that the CO_2 probably plays an important role in the particle growth during the thermal decomposition of magnesite. However, there is no enough evidence to exclude the impact of the vacuum itself on the grain growth. Therefore, further studies of grain growth were carried out in CO_2. The particle size was smaller in CO_2 than in air as well, which indicated that there were almost no effects on the

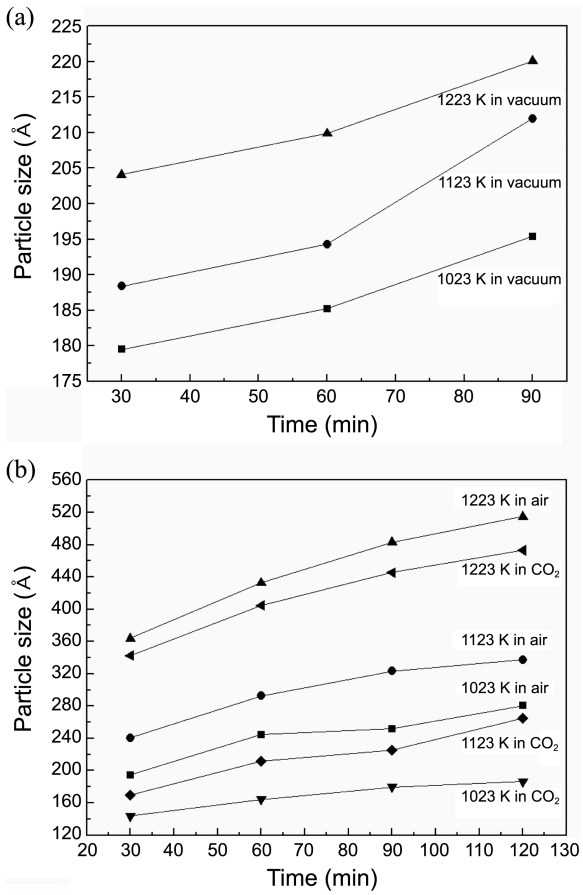

Figure 5. Particle size of MgO prepared in different environments. (a) in vacuum (b) in air and in CO_2.

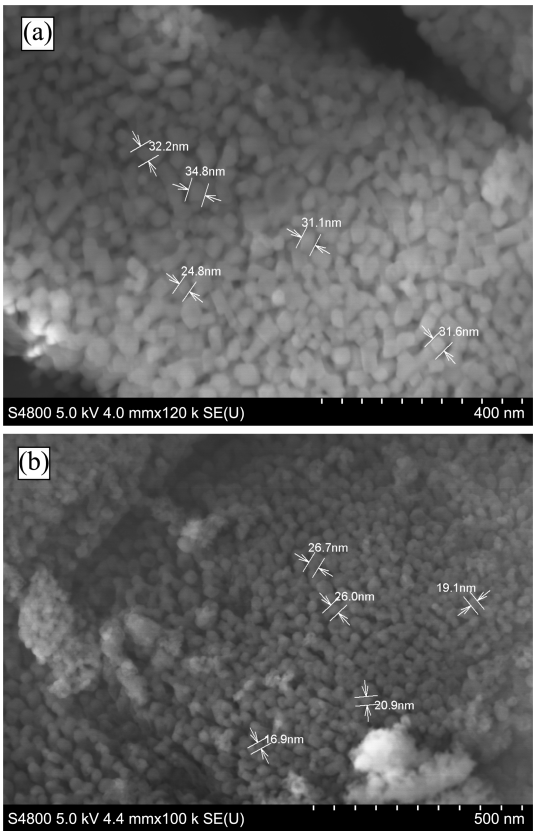

Figure 6. The SEM micrographs of the specimens prepared at 1123 K for 60 min. (a) in air; (b) in vacuum.

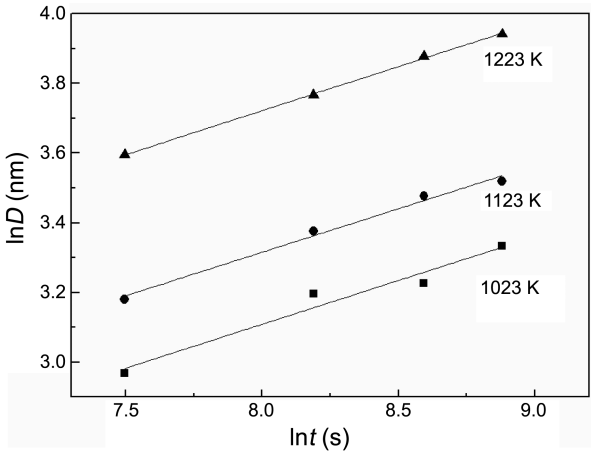

Figure 7. The plot of ln$D$ *vs* ln$t$ for MgO particle growth in air.

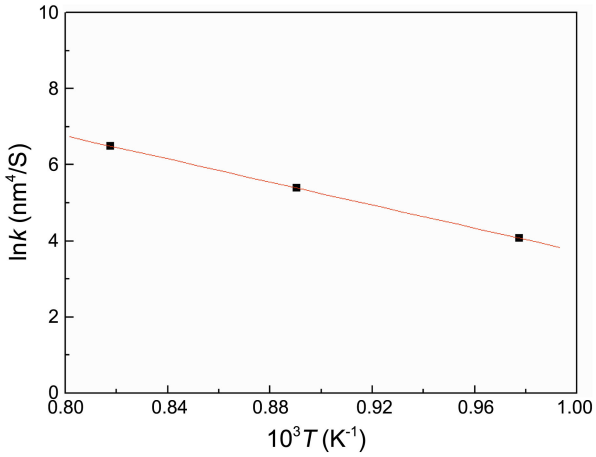

Figure 8. The plot of ln$k$ *vs* 1/T for the particle growth of MgO in air.

grain growth in CO_2. This result was in agreement with the previous report.[24] The specimens both prepared in air and vacuum at 1123 K for 60 min were observed by SEM, as can be seen in Figure 6. The particle surface of MgO which was calcined in air has been sintered, while the grain boundaries of the specimen which was prepared in the vacuum were still clear. In Figure 6(a) and Figure 6(b), the size of five randomly selected particles were measured. The mean particle size are 30.9 nm in Figure 6(a) and 21.9 nm in Figure 6(b), respectively. This result is agreement with the calculated value.

Discussion

As this article's aim is to study the mechanism of grain growth in air, in this case only the particle growth of MgO in air was considered. The results of isothermal particle growth in air are shown in Figure 7 as a ln$D$ - ln$t$ plot, in which the values of n and k were obtained by using the grain growth equation $D^n = kt$, where D is the particle size, k is the rate constant, t is the time, n is a coefficient.

The value of n remained constant (about 4) in the whole temperature range studied. According to the Arrhenius equation, k can be expressed as:

$$k = k_0 \exp\left(-\frac{Q}{RT}\right) \quad (3)$$

A plot of ln k *vs* 1/T is shown in Figure 8. The activation energy and pre-exponential factor were calculated to be 125789 ± 161 J/mol, (1.56 ± 0.03) × 10^8 nm^4/s, respectively.

In discussing operative mechanisms in the particle growth process during the thermal decomposition of magnesite the following facts are considered. The activation energy of the particle growth during the calcined magnesite in air is about 125.8 kJ/mol which is much lower than that of bulk diffusion and surface diffusion. The activation energy of bulk diffusion for Mg^{2+} in MgO from 973 K to 1573 K is about 231 kJ/mol[25] and that for O^{2-} in MgO from 1121 to 1248 K is approximately 279 kJ/mol.[26] The activation energy of surface diffusion of MgO is 376.7 kJ/mol.[11]

Analogous to the reasons that the activation energy is much lower in H_2O vapor than that of bulk diffusion and surface diffusion, maybe some kinds of surface structure are formed between CO_2 and MgO during the thermal decomposition of magnesite. In this paper, these surface structures

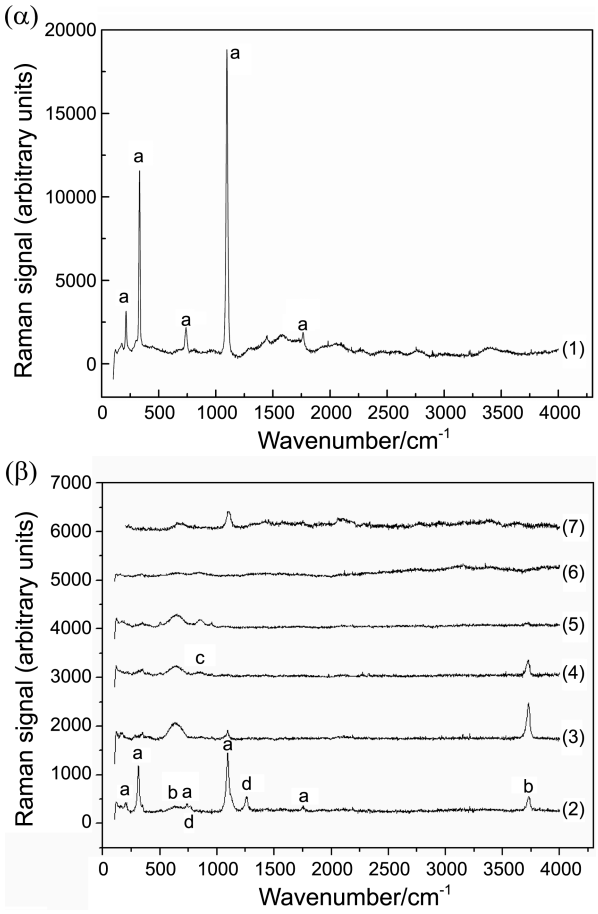

Figure 9. Raman spectrum during the thermal decomposition of magnesites. (α) includes spectrum (1); (β) includes spectrum (2)-(7). Specific: (1) at room temperature; (2) 773 K; (3) 823 K; (4) 873 K; (5) 923 K; (6) 973 K; (7) the MgO sample was sealed in CO_2 for 30 minutes. all bands are classified into the four groups: a (the first group); b (the second group); c (the third group); d (the fourth group).

were studied by Raman spectrum which was shown in Figure 9.

In spectrum (1) where the sample of magnesite was observed at room temperature, the brands appeared at 214, 332, 1096 cm^{-1} with very weak bands at 739, 1764 cm^{-1}. These peaks were not changed until 773 K. In spectrum (2), the new bands appeared at 3728, 1256 cm^{-1} with very weak bands at 638, 764 cm^{-1}. The bands at 1256, 764 cm^{-1} disappeared in spectrum (3) which was measured at approximately 823 K. As the temperature was continually increased, the bands at 214, 332, 1096, 739, 1764 cm^{-1} decreased greatly in intensity and disappeared at approximately 873 K. The new bands at 848 cm^{-1} was observed in spectrum (4). All bands disappeared at 973 K. The spectrum (7), where the bands were observed at 638, 1096 cm^{-1}, shows the surface structure result of the MgO sample which was sealed in CO_2 for 30 minutes.

In Figure 9, all bands can be classified into the following four groups. The first group includes the bands at 214, 332, 1096, 739, 1764 cm^{-1}, which were obtained at room temperature from the sample of magnesite. The CO_3^{2-} could be assigned at these vibrational frequencies. The second group includes the bands at 638, 3728 cm^{-1}, which appeared in spectrum (2)-(5). Compared to the spectrum (7), these bands must be correlated with the adsorption of CO_2. According to Philipp and Fujimoto,[19] the unidentate is predominantly formed at room temperature. Therefore, the unidentate carbonates can be assigned to this group. The third group includes the bands at 848 cm^{-1}, which appeared in spectrum (4) and the intensities increased in spectrum (5). In spectrum (4), the disappearing bands of CO_3^{2-} indicate that the amount of adsorbed CO_2 was reduced. According to Fukuda and Tanabe,[16] both unidentate and bidentate carbonates are formed on MgO when a small amount of CO_2 is adsorbed and unidentate carbonates predominate with the increasing amount of adsorbed CO_2. So, the bidentate carbonates may be assigned to the third group. On the other hand, several papers[15-17] attributed the bidentate carbonates to the bands at 850 cm^{-1} of infra-red spectrum. If the bidentate carbonates are both Raman active and infra-red active, this may provide another reason for the bidentate carbonates to be assigned to the bands at 850 cm^{-1}. The fourth group includes the bands at 764, 1256 cm^{-1}, which appeared in spectrum (2) and disappeared in spectrum (3). It is still not well understood so far.

Based on the above analysis, the mechanism of grain growth can be speculated as follows:

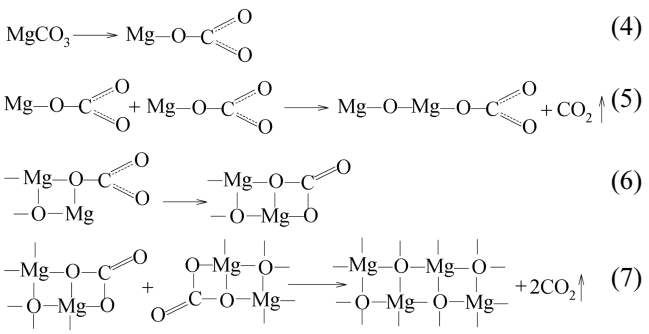

(4)

(5)

(6)

(7)

Eqs. (4) and (6) indicate the formation of the unidentate and bidentate carbonates, respectively. The effects of the unidentate and bidentate carbonates on the grain growth of MgO are expressed by Eqs. (5) and (7), respectively. From Eq. (4), it is obvious that the productions of the calcined magnesite are not direct MgO and CO_2, but a kind of intermediate combined of MgO with the adsorption of unidentate carbonates. One the one hand, the intermediate still exists above the decomposition temperature of $MgCO_3$. On the other hand, although several workers have reported that active MgO can absorb CO_2, all these experiments were carried out in CO_2 atmosphere, while in this work, the magnesite was calcined in air that indicated the low partial pressure of CO_2. Therefore, it can be easily deduced that there is a kind of highly reactive MgO in the intermediates, which can adsorb CO_2 at high temperature and lower partial pressure of CO_2. The existence of this kind of highly reactive MgO has been supposed by Kwon and Park[27] in their papers though its thermodynamic parameters are not well understood. From Eq. (5), it can be seen that the chemical bond A breaks and the CO_2 of a unit is produced during the grain growth. After the complete decomposition of magnesite, the less and less amount of CO_2 is on the surface of MgO that lead to the changes from unidentate carbonates to bidentate carbonates as be shown by Eq. (6). The growth process of the grain with the adsorption of bidentate carbonates is expressed as Eq. (7) from which the chemical bonds both C and D break and the CO_2 of two units are produced at the same time.

According to these equations, the reasons of the lower activation energy of grain growth during the thermal decomposition of magnesites may be attributed to the formation of oxygen bridges. However, this mechanism cannot well explain the following facts.

(1) From the Raman spectrum (6) in Figure 9, it can be found that the bands of these surface structures disappeared at 973 K. This result indicates that these surface structures are unstable at the experimental temperature. On the other hand, the decomposition rate of magnesite is very fast that only about 10 min is necessary for completing the decomposition reaction at the experimental temperature. In other words, the effects of CO_2 produced from the decomposition of magnesite on the grain growth of MgO are only in the initial few minutes.

(2) The activation energy of grain growth in H_2O vapor is nearly the same as that of grain growth during the thermal decomposition of brucite,[7,8] while according to this paper, there is no effect on the grain growth of MgO in CO_2.

(3) In H_2O vapor, it can form the surface hydroxyl groups on MgO, which can be classified as the chemical adsorption whereas a kind of physical adsorption occurs in the existence of CO_2. However, with the different adsorption mechanism, the activation energy of grain growth for the both kinds of adsorption is nearly the same, which is 130 kJ/mol and 125.8 kJ/mol, respectively. Therefore, it cannot well explain this reason by using the mechanism of the activation energy decreasing resulting from the adsorption structures.

According to the above analysis, a new mechanism can be expressed as follows:

(1) The surface structure on MgO formed due to the adsorption of either CO_2 or H_2O enables the ordered grain growth with crystals having fewer defects, but contributes little to the activation energy decreasing;

(2) The most important reason for activation energy decreasing is due to the existence of highly reactive MgO.

The following facts can be well explained by using this mechanism.

(1) The activation energy of grain growth for the thermal decomposition of magnesite and brucite is so similar, which is 133.9 kJ/mol and 125.8 kJ/mol, respectively. This result indicates that there is the same mechanism of grain growth for the thermal decomposition of magnesite and brucite since the highly reactive MgO is produced in both of the decomposition processes.

(2) In H_2O vapor, the dynamic equilibrium reaction occurs as follows:

$$MgO + H_2O \leftrightarrow Mg(OH)_2 \quad (8)$$

The effect of water vapor on grain growth of MgO is to regain the highly reactive MgO by chemical reaction. It can well explain why the activation energy of grain growth in H_2O vapor is almost the same in comparison with that of the thermal decomposition of magnesite and brucite.

(3) In CO_2 atmosphere, MgO cannot occur chemical reaction as in H_2O vapor. In other words, at the experimental temperature, the following reaction cannot occur:

$$MgO + CO_2 \rightarrow MgCO_3 \quad (9)$$

There is no the highly reactive MgO produced in this process. Therefore, there is no effect on the grain growth of MgO in CO_2.

From this paper, it can be found that the better the activation of MgO is, the larger grain size of MgO is on the same conditions. Therefore, this may be a possible way to understand the activity of materials by means of comparing the size of grain growth in the same processing conditions, which can be only determined by further experiments.

Summary and Conclusions

In this paper, the grain size of MgO either in CO_2 or during the thermal decomposition of magnesites in air as well as in vacuum was calculated at 1023 K, 1123 K and 1223 K respectively. By referring to the conventional grain growth equation: $D^n = kt$, the activation energy and pre-exponential factor for the process in air are gained as 125.8 kJ/mol and 1.56×10^8 nm^4/s, respectively.

The surface structure of the obtained MgO during calcination of magnesite was studied by Raman spectroscopy, and the mechanism of grain growth can be expressed as follows:

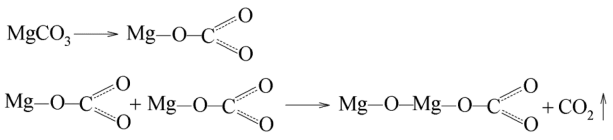

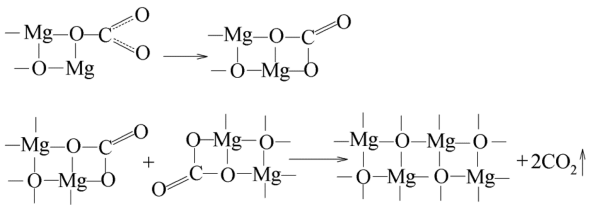

It is suggested that a kind of highly reactive MgO is produced during the thermal decomposition of magnesites. This kind of highly reactive MgO is believed to be the reason of the lower activation energy of grain growth than that of bulk diffusion or surface diffusion compared with the process of MgO growth in H_2O vapor, in CO_2 atmosphere and in air. At the same time, it may be a possible way to understand the activity of materials by means of comparing the size of grain growth in the same conditions.

Acknowledgments. The authors would like to thank Xianwei Hu for his help in analytical characterization of Raman spectrums. We would also like to thank Jianping Peng and Yuezhong Di for the suggestions in this paper.

References

1. Turčániová, L'.; Paholič, G.; Mateová, K. *Thermochim Acta* **1996**, *277*, 75.
2. Rocha, S. D. F.; Mansur, M. B.; Ciminelli, V. S. T. *J. Chem. Technol. Biotechnol.* **2004**, *79*, 816.
3. Birchal, V. S. S.; Rocha, S. D. F.; Ciminelli, V. S. T. *Miner. Eng.* **2000**, *13*, 1629.
4. Birchal, V. S. S.; Rocha, S. D. F.; Mansur, M. B.; Ciminelli, V. S. T. *Can. J. Chem. Eng.* **2001**, *79*, 507.
5. Gordon, R. S.; Kingery, W. D. *J. Am. Ceram. Soc.* **1966**, *49*, 654.
6. Kim, M. G.; Dahmen, U.; Searcy, A. W. *J. Am. Ceram. Soc.* **1988**, *71*, 373.
7. Kotera, Y.; Saito, T.; Terada, M. *Bull. Chem. Soc. Jpn.* **1963**, *36*, 195.
8. Aihara, K.; Chaklader, A. C. D. *Acta Metall.* **1975**, *23*, 855.
9. Lindner, R.; Partitt, G. D. *J. Chem. Phys.* **1957**, *26*, 182.
10. Oishi, Y.; Kingery, W. D. *J. Chem. Phys.* **1960**, *33*, 905.
11. Robertson, W. M. Gordon and Breach: New York, 1967; p 215.
12. Fubini, B.; Bolis, V.; Bailes, M.; Stone, F. S. *Solid State Ionics* **1989**, *32-33*(1), 258.
13. Anderson, P. J.; Morgan, P. L. *Trans. Faraday Soc.* **1964**, *60*, 930.
14. Razouk, R. I.; Mikhail, R. S.; Ragai, J. J. *Appl. Chem. Biothchnol.* **1973**, *23*, 51.
15. Evans, J. V.; Whateley, T. L. *Trans. Faraday Soc.* **1967**, *63*, 2769.
16. Fukuda, Y.; Tanabe, K. *Bull. Chem. Soc. Jpn.* **1973**, *46*, 1616.
17. Stark, J. V.; Park, D. G.; Lagadic, I.; Klabunde, K. J. *Chem. Mater.* **1996**, *8*, 1904.
18. Philipp, R.; Omata, K.; Aoki, A.; Fujimoto, K. *J. Catal.* **1992**, *134*, 422.
19. Philipp, R.; Fujimoto, K. *J. Phys. Chem.* **1992**, *96*, 9035.
20. Cao, P.; Lu, L.; Lai, M. O. *Mater. Res. Bull.* **2001**, *36*, 981.
21. Zhou, L. Z.; Guo, J. T. *Scripta Mater.* **1999**, *40*, 139.
22. Elkind, A.; Barsoum, M. W. *J. Mater. Sci.* **1996**, *31*, 6119.
23. Lewis, D.; Pearson, H. *Nature* **1962**, *196*, 162.
24. Varela, J. A.; Whittemore, O. J.; Longo, E. *Ceram. Int.* **1990**, *16*, 177.
25. Sakaguchi, I.; Yurimoto, H.; Sueno, S. *Solid State Commun.* **1992**, *84*, 889.
26. Oishi, Y.; Ando, K.; Yasumura, K. J. *Am. Ceram. Soc.* **1987**, *70*, C327-C329.
27. Kwon, H.; Park, D. G. *Bull. Korean Chem. Soc.* **2009**, *30*, 2567.